Review of Fluorescence Suppression Techniques in Raman Spectroscopy

Dong Wei, Shuo Chen & Quan Liu

Taylor & Francis
Taylor & Francis Group

Review of Fluorescence Suppression Techniques in Raman Spectroscopy

DONG WEI, SHUO CHEN, AND QUAN LIU

School of Chemical and Biomedical Engineering, Nanyang Technological University, Singapore

Abstract: *Raman spectroscopy is an important and powerful technique for analyzing the chemical composition of biological or nonbiological samples in many fields. A serious challenge frequently encountered in Raman measurements arises from the existence of the concurrent fluorescence background. The fluorescence intensity is normally several orders of magnitude larger than the Raman scattering signal, especially in biological samples. Such fluorescence background must be suppressed in order to obtain accurate Raman spectra. Several different techniques have been explored for this purpose. These techniques could be generally grouped into time-domain, frequency-domain, wavelength-domain, and computational methods in addition to various Raman enhancement techniques and other unconventional methods. This review briefly describes the fundamental principles of each group of methods, reports the most recent advances, and makes comparison across those major categories of techniques in terms of cost and performance in a hope to guide interested readers to select proper methods for specific applications.*

Keywords: Raman spectroscopy, fluorescence suppression, time-domain optical methods, frequency-domain optical methods, wavelength-domain optical methods, computational methods for fluorescence background removal

Introduction

Raman spectroscopy relies on the inelastic scattering of a sample upon light radiation, which can be utilized to detect vibrational, rotational, and low-frequency modes in a system (1, 2). It is a very important tool to investigate the property changes of materials, such as phase transitions (3), polymorphs (4), and crystallinity (5). Because of its noninvasiveness and high chemical specificity, this technique is also ideal for the characterization of biological samples. For example, Raman spectroscopy has been explored in cell studies (6–8), tropical disease diagnosis (9, 10), cancer diagnosis (11–13), dentistry (14), etc. Raman spectroscopy has many advantages over other common analytical techniques, including high spatial resolution, less harmful near-infrared radiation, minimum sample preparation, reduced influence of water bands, and high chemical sensitivity, which allow both in vitro and in vivo analyses (15). Moreover, Raman spectroscopy can be used to study solid, liquid, and gaseous samples.

However, a serious problem in most applications of Raman spectroscopy is the strong fluorescence background, which is partially attributed to the low cross section of Raman

Address correspondence to Quan Liu, School of Chemical and Biomedical Engineering, Nanyang Technological University, Block N1.3, 70 Nanyang Drive, Singapore 637457. E-mail: quanliu@ntu.edu.sg

scattering. Many Raman active molecules also exhibit fluorescence upon excitation in conventional Raman spectroscopy, which can be frequently encountered in a complex sample. Moreover, fluorescence photons could induce a strong background and also raise the overall shot noises (16), masking much weaker Raman signals. In contrast to the weak Raman signal, strong fluorescence background renders Raman spectral acquisition difficult and results in long acquisition time.

Fluorescence occurs concurrently with Stokes Raman scattering upon laser excitation because the red-shifted Stokes Raman scattering would spectrally overlap with fluorescence emission. The fluorescence problem does not exist for anti-Stokes Raman scattering because anti-Stokes Raman scattering is blue shifted compared to the excitation wavelength and thus is naturally separated from fluorescence in the spectrum. The fluorescence background problem is more serious when visible light is used for excitation. The strong fluorescence signal in Raman spectroscopy directly affects the accuracy and sensitivity of Raman measurements. In the past decade, a variety of hardware- and software-based methods have been proposed for quenching fluorescence background and enhancing weak Raman signals. One simple method is to use near-infrared wavelength light as the excitation source, in which case the excitation energy is generally insufficient to excite strong fluorescence. Thus, the molecules will emit less fluorescence compared to the case of using excitation light at a shorter wavelength (17). However, this method is less effective in biological samples, in which more sophisticated methods have been explored. In this review article, the major categories of experimental methods for fluorescence suppression are described in detail and major algorithms for the same purpose are briefly introduced. The potential future directions of development in fluorescence suppression techniques are discussed at the end.

Major Categories of Methods for Fluorescence Suppression

Fluorescence and spontaneous Raman signals overlap in the wavelength dimension and thus cannot be separated using simple optical filters. Fortunately, they differ from each other in the following properties, which form the bases of many methods for fluorescence suppression in Raman measurements:

1. The lifetime of fluorescence emission (on the order of nanoseconds) is much longer than that of Raman scattering (on the order of picoseconds). This principle yields various time-domain methods in which an ultrafast pulse laser is used for excitation (18–20).
2. The difference in lifetime between fluorescence and Raman signals could be translated into a larger phase delay and amplitude demodulation in fluorescence compared to Raman signals when the excitation light is modulated at a high frequency. This principle is the basis for all frequency-domain methods (21–23).
3. The wavelength of a Raman peak changes with the excitation wavelength, whereas the much broader fluorescence peak is insensitive to the excitation wavelength. This property has led to various wavelength-domain methods such as shifted excitation Raman difference spectroscopy (SERDS) (15, 24).
4. Raman peaks are much narrower in bandwidth than fluorescence peaks. This property leads to various algorithm-based baseline correction methods for fluorescence background removal after data acquisition (25–29).
5. Fluorescence background will be efficiently quenched and the Raman signal will be dramatically enhanced when a molecule is in direct contact with the metal

nanoparticles. This fact has resulted in the rapid development of surface-enhanced Raman spectroscopy (SERS) (30, 31). SERS could enhance or deteriorate fluorescence emission intensity by interaction between fluorophore and metal nanoparticles (NPs), depending on the shape of NPs, the orientation of the fluorophore's molecular dipolar moment, and the fluorophore emission spectrum overlapping with the spectrum of NPs' surface plasma resonance (32).
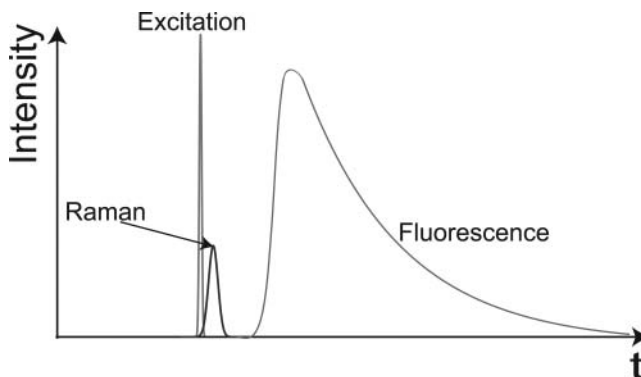
6. The Raman signal can be greatly enhanced to dominate over fluorescence when the frequency of the excitation light is close to the electronic transition of the molecule. This phenomenon is due to the spectroscopic selection rule of Raman spectroscopy, which leads to resonance Raman spectroscopy (33–35). Some nonlinear techniques such as coherent anti-Stokes Raman spectroscopy (36) and stimulated Raman spectroscopy (SRS) (37) can also dramatically enhance Raman signals while minimizing the fraction of detected background fluorescence.

7. Other methods used to suppress fluorescence include polarization gating (38), sampling optics and geometries (39, 40), photobleaching (41, 42), etc.

This review will focus on methods in categories 1 through 4 as well as 7 for spontaneous Raman spectroscopy. For the rest of methods, readers are referred to the respective review papers in the literature given above.

Time-Domain Methods

Time-domain techniques require ultrashort laser pulses (2, 43). This category of methods takes advantage of the different response of Raman scattering and fluorescence background signal in the timescale (44) in which fluorescence has a much longer lifetime (approximately hundreds of picoseconds to a few nanoseconds) than the Raman signal (picoseconds to femtoseconds). It should be noted that laser pulses should not be too short because pulses shorter than 1 ps are less monochromatic, which will result in serious loss of spectral resolution. The quickly arriving Raman scattered light from late-arriving fluorescence emission of a sample excited by ultrafast optical pulse trains could be temporally separated.

Figure 1 illustrates the temporal profile of the excitation laser pulse, emitted Raman scattering signal, and emitted fluorescence. The fluorescence process consists of three important steps according to a Jablonski diagram (2), in terms of excitation, internal conversion, and emission, each of which occurs at a different timescale (2). Firstly, the excitation of fluorophore molecules by incoming photons occurs on the order of femtoseconds (10^{-15} seconds). Secondly, the nonradiative internal conversion process through vibrational relaxation is also very fast, between 10^{-14} and 10^{-11} s. Finally, fluorescence emission is a slow process occurring on the order of 10^{-9} to 10^{-7} s. The fluorescence lifetime refers to the average time the molecule stays on its excited state before emitting a fluorescence photon. The exponential decay curve shown in Figure 1 illustrates the statistical distribution of time taken for fluorescence emission. The fluorescence temporal profile I(t) could be fitted to an exponential function a lifetime constant τ for a single fluorophore, according to $I(t) \propto e^{-t/\tau}$, whereas the Raman emission occurs nearly simultaneously with the excitation laser light. Because the Raman signal is emitted much faster than fluorescence, a well-chosen temporal gate with an appropriate gate width will be able to detect Raman signals while minimizing the fluorescence contribution in principle.

Figure 1. Temporal profile of the excitation laser pulse, emitted Raman scattering signal, and emitted fluorescence. The fluorescence intensity decays exponentially with its lifetime, whereas the Raman emission occurs nearly simultaneously with the excitation laser pulse.

A variety of time-domain methods have been established, which can be based on the Kerr gate (45), photomultiplier tubes (46), intensified charge-coupled device cameras (47, 48), complementary metal oxide semiconductor (CMOS) detectors (16), and streak cameras (49). These representative methods will be described in this following.

A useful technique removes fluorescence from a Raman signal with an optically driven Kerr gate (45, 50, 51). A Kerr gate is composed of a nonlinear Kerr medium between two crossed polarizers. The nonlinear interaction of the Kerr medium with a high-energy gating laser pulse induces a transient anisotropy due to the optical Kerr effect, which allows any incident linearly polarized light to rotate its polarization by 90°. By synchronizing the gating laser pulse with the excitation laser for Raman measurements, Raman light can pass through the cross-polarizer because the Kerr medium acts as a half-wave plate and the polarization of the Raman light is rotated by 90°. But fluorescence, which has a longer lifetime and thus is not synchronized with the gating laser pulse, is efficiently blocked between two crossed polarizers. An effective Kerr gate should possess a fast gating time and high transmission for Raman light.

Picosecond time-domain Raman spectroscopy technique with a Kerr gate could experimentally achieve fluorescence rejection in measured Raman spectra. The Kerr gate had a response time of around 3 ps when driven by 10 μJ, 1 ps excitation pulses at a wavelength of 800 nm and a repetition frequency of 0.65 KHz (45). However, due to the incomplete polarization rotation in the Kerr medium and losses in optical elements, the optical transmittances of the Kerr gate in the open and closed state were only 15 and 0.005%, respectively. Matousek et al. (50) reported an improved Kerr gate with optimized polarizers, which showed a 4-ps gate open time when operated under 1 ps pulse laser with 1 kHz overall repetition rate. The throughput in the open state was improved up to ~40% and the extinction ratio between the open and closed state was boosted to 10^5. As the result of more efficient gating, the overall transmission and the collection efficiency of Raman light reached up to 1.6 times and 1.7 times, respectively, relative to their earlier results (45). Using Kerr-gated picosecond time-resolved Raman spectroscopy, light penetration through an equine cortical bone tissue to reach a depth of 0.3 mm was shown to be feasible with 1-ps pulsed laser excitation at a wavelength of 400 nm and a frequency of 1 kHz (51). However, the Kerr gate method has not found widespread use

in the investigation of biological samples due to the need for excessively high-energy pulsed light sources, increasing photo-induced damage risk (47).

Another time-domain method is to directly utilize an ultrafast time-gated detector for Raman detection to suppress fluorescence (47–49). There are two key parameters for this method. One is a short gate width and the other is a sufficiently high repetition rate to maintain an acceptable detector duty cycle (52). With a proper time gate, typically on the order of a few hundred picoseconds, Raman signals could be detected efficiently while fluorescence is largely suppressed as described below, where a photomultiplier tube, an intensified charge-coupled device (CCD) camera, or a CMOS single-photon avalanche detector (SPAD) served as the time-gated detector.

In order to reject background fluorescence, a single photon counting technique using a single-channel gated detector has been implemented with short-duration (~5 ps), highly repetitive rate (~82 MHz) pulsed laser and a microchannel plate–type photomultiplier (with a time gate width of 31 ps), which was used to suppress fluorescence from a sample of rhodamine 6G in ethanol (46). The signal-to-noise ratio of the Raman signal and Raman-to-fluorescence intensity ratio were dramatically improved by factors of 4.2 and 129, respectively, compared to the case of without gating. Another Raman system whose cost was relatively low included a pulsed diode laser with 6.4 kHz repetition rate and 900 ps pulse width and a photomultiplier tube for time-resolved photon counting (53). This system demonstrated that the signal-to-noise ratio for a neat benzene sample doped with rhodamine 6G at a concentration of 10^{-4} M was approximately improved by 15-fold when a short gate width (0.7 ns) was used in time-resolved photon counting relative to a long one (25 ns).

Gated single-channel detectors, such as photomultipliers and photodiodes, have been gradually replaced by two-dimensional (2D) detector arrays such as the intensified charge coupled device camera, CMOS detectors, and streak cameras to improve spectral quality. These 2D arrays enable the simultaneous acquisition of a few Raman bands each time, resulting in more efficient measurements of the whole spectrum (16).

Martyshkin et al. (47) utilized a mode-locked laser together with an intensified CCD camera to effectively perform time-gated suppression of fluorescence from hexabenzo-coronene and long-lived fluorophore from Nd^{3+} impurity. When the time-gated detector was switched on after an appropriate time delay, it was possible to effectively discriminate Raman photons originating from different depths (19). The intensified gated CCD camera was operated at 110 MHz repetition rate and a temporal gate width of about 150 ps under 785-nm pulsed laser excitation that had a 76-MHz repetition rate and 2-ps pulse duration. In another study, a pulsed 532-nm laser excitation source and an electronic gate CCD detector synchronized with the laser were used to suppress impurity-induced and stress-induced fluorescence in diamond (20). The system allowed the suppression of undesired incandescent radiation that showed up as wide and spectrally continuous light by a factor of up to 50,000 and acquired Raman signals at a temperature above 5000 K and a high pressure near 150 GPa.

Furthermore, the CMOS SPAD with a gate time width shorter than 100 ps has been used to reduce the fluorescence background on olive oil samples (16). The CMOS SPAD is a 2D array, and its time gate is very short (less than 100 ps). However, this technique has two limitations. One is that the CMOS SPAD detector has only modest photon detection efficiency, and the other is its low fill factor, which could affect the SPAD's sensitivity and capability to effectively capture Raman photons, especially in the near-infrared region (16). Alternatively, a picosecond pulsed laser together with a streak camera is another choice to reject fluorescence in the time domain (49). The advantages of using a
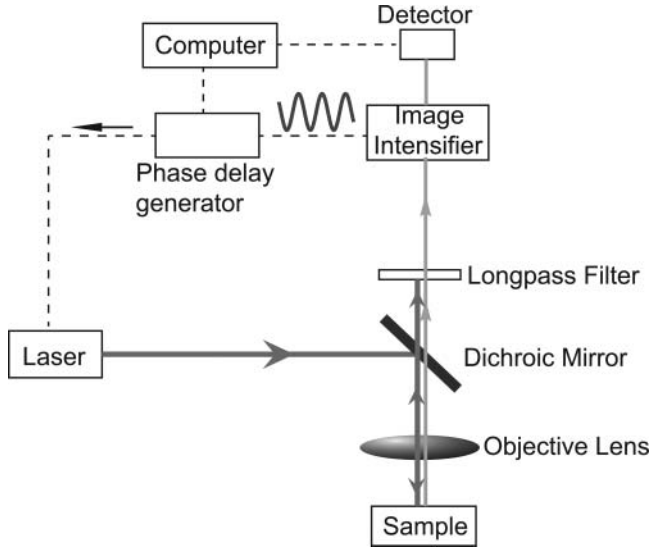
streak camera include its high time resolution as short as 10 ps, making deconvolution unnecessary, and two-dimensional capability, allowing for multichannel detection. The latter advantage enables the gated detection to be performed simultaneously at multiple wavelengths, which greatly reduces measurement time and reduces the complexity of the detection system. Using this approach, an improved Raman-to-fluorescence intensity ratio of 281 was achieved in the measurement of a solution mixing benzene and rhodamine 640 fluorophore. Comparing all of the above-mentioned 2D detector arrays including the gated CCD, CMOS, and streak camera, the CMOS camera has an advantage in cost compared to the CCD (54) and streak camera (55); furthermore, CMOS offers advantages in integration, power dissipation, and system size compared to the CCD (54). However, the CCD and streak camera offer superior image quality and high signal-to-noise ratio for photon detection in the near-infrared region at the expense of the camera size, compared to a highly integrated CMOS camera (56).

Frequency-Domain Methods

The second category of methods for suppressing fluorescence in Raman measurements is the frequency-domain method (21–23, 57), which is sometimes called the phase-modulation method (2). The time-domain and frequency-domain methods are related to each other by the Fourier transform. Furthermore, the frequency-domain methods could measure fluorescence lifetime at the same time while reducing the fluorescence. There are two common types of frequency-domain methods. One is frequency domain demodulation (57) and the other is frequency-domain phase nulling (22, 23, 58, 59). Both types of methods can be used to suppress fluorescence in Raman measurements.

The principle of the frequency domain demodulation method is rooted in the different behaviors in the response between fluorescence and Raman scattering under high-frequency modulation. When a high-frequency sinusoidal waveform is used for excitation, fluorescence that behaves like a low-pass filter cannot follow the high-frequency modulation, resulting in amplitude demodulation and phase shift relative to the excitation light. In comparison, Raman scattering can instantaneously follow the high-frequency modulation of the excitation light. The Raman and fluorescence signals that were collected by a photomultiplier detector in combination with a microwave spectrum analyzer can be discriminated by extracting the high-frequency (mostly Raman) or low-frequency (mostly fluorescence) components from the output of the detector. Therefore, the approach of the frequency domain demodulation method can be employed to resolve the sample's scattering contribution while minimizing the interference from fluorescence (57). Bright and Hieftje demonstrated that strong fluorescence ground from rhodamine 6G could be suppressed from Raman signals using the frequency-domain demodulation method. The long-lived fluorescence with a lifetime of 3.6 ns was demodulated using a modulation frequency at 328 MHz while the Raman scattering was strongly modulated. As a result, the fluorescence was rejected by a factor of 7 (57).

The other type of frequency-domain methods—that is, frequency-domain phase nulling—will be described in detail in the following. In a general frequency-domain phase-nulling setup (Figure 2) (60), a sample is illuminated with sinusoidally modulated light at an angular frequency ω produced by a function generator built in a gain-modulated image intensifier. The resulting Raman/fluorescence signal that passes through a dichroic mirror and a long-pass filter is modulated at the same angular frequency but with different time delays, which is detected by a gain-modulated image intensifier with the same modulation frequency ω and a detector coupled to the intensifier. The phase delay between the laser

Figure 2. General schematic of a frequency-domain phase-nulling system for fluorescence suppression. Red and orange solid lines represent the flow of optical signals; black dashed lines represent the flow of electronic signals.

modulation and the gain modulation of the image intensifier can be set electronically by the phase-delay generator.

At different phase delays, a series of images including the contributions of both fluorescence and Raman emission are taken. For fluorescence alone, the modulation depth m and phase shift ψ_F compared to the excitation light are related to the fluorescence lifetime τ, assuming a single fluorophore, in the following manner mathematically (2):
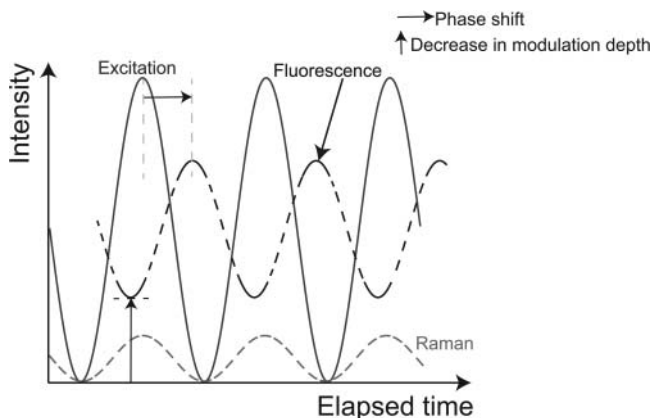
$$m = \frac{1}{\sqrt{1 + \omega^2 \tau^2}} \text{ and } \psi_F = \tan(\omega\tau). \tag{1}$$

The phase shift ψ_F developed between the fluorescence and laser excitation and the modulation depth m in the time domain are illustrated in Figure 3. Fluorescence lags behind the excitation light while the Raman signal is almost in phase with the excitation light. In addition, the modulation depth of the Raman signal is nearly identical to that of the excitation light because the extremely short lifetime of Raman scattering determines its modulation depth close to 1 according to Eq. (1). Supposing that a two-component sample consists of a Raman scatterer and a single fluorophore, the resulting frequency-domain intensity $I(\psi_D, \lambda)$ can be expressed as (61):

$$I(\psi_D, \lambda) = F(\lambda) m_{ex} m_F \cos(\psi_D - \psi_F) + R(\lambda) m_{ex} m_R \cos(\psi_D - \psi_R), \tag{2}$$

where ψ_D is the phase angle generated by the phase-delay generator; $F(\lambda)$ and $R(\lambda)$ are the fluorescence spectrum and Raman spectrum, respectively; ψ_R is the phase shift for the Raman signal, which is approximately zero; m_{ex} is the modulation depth of the excitation laser; and m_F and m_R are the modulation depthsof the fluorescence and Raman signals,

Figure 3. In the frequency-domain method where the excitation light is modulated, considerable phase shift and modulation depth change can be observed between fluorescence emission (black dashed line) and excitation light (blue solid line), whereas there is only a negligible phase shift and very small modulation depth change between Raman scattering (red dashed line) and excitation light (blue solid line). The horizontal arrow "→" shows the phase shift between the excitation light and fluorescence emission, and the vertical arrow "↑" indicates the decrease in modulation depth from the excitation light to fluorescence emission.

respectively. Note that the latter modulation depth is approximately equal to 1 due to the extremely short lifetime of Raman scattering.

The fluorescence may be suppressed by setting the phase angle ψ_D equal to $\psi_F \pm 90°$ to null the fluorescence signal. The resulting signal becomes

$$I(\psi_D, \ \lambda) = \ R(\lambda)m_{ex}m_R\sin(\psi_F - \psi_R), \tag{3}$$

which indicates that the detected signal is only proportional to the Raman contribution.

The frequency-domain phase-nulling method, which was frequently used to measure phase shift and modulation depth to resolve the components of fluorescence species in a mixture based on known decay times, can be used to suppress fluorescence as shown in Eq. (3). The Raman and fluorescence signals from the sample can be detected separately with a lock-in amplifier also known as a phase-sensitive detector by setting an appropriate phase delay. The phase-sensitive detector essentially implements Eq. (3) in a single unit. When the detector is set as out of phase (90°) with respect to the fluorescence emission, fluorescence is totally suppressed in theory. In this manner, the fluorescence-free signal is obtained with a minimal decrease in the Raman signal (22, 23). Furthermore, the analysis of measured phase-sensitive data using a nonlinear least-squares algorithm could yield the fractional intensities and lifetimes of individual fluorescence species in the mixture (62).

For a sample with two components each having a different lifetime, the phase-resolved background suppression technique, which is essentially one of frequency-domain methods, could totally suppress fluorescence from one component and partially attenuate the other by use of a phase-sensitive detector. For example, Demas and Keller used a phase-sensitive detector and an excitation light source modulated at 40 MHz to separate the Raman signal of water from rhodamine 6G fluorescence with a lifetime of 3 ns (22). In the same study, by adding a lock-in amplifier, luminescence from [Ru

$(bpy)_3]^{2+}$ with a longer lifetime of 350 ns can also be separated from water Raman scattering or rhodamine fluorescence (22). Wirth and Chou (23) compared the frequency- and time-domain methods for quenching fluorescence from Raman spectra. By operating at a high modulation frequency of 329 MHz, the frequency domain method could enhance the Raman signals value by 200 times and significantly improve the performance in fluorescence suppression. In comparison, the time-domain method can only achieve lower fluorescence rejection in the study. However, the frequency modulation method required a quite complicated system for fluorescence suppression and could not easily reduce the statistical noise. Furthermore, the frequency modulation method did not work well for separating fluorescence from a Raman spectrum over a large spectral range (23). Rusciano et al. described a new technique that removed the fluorescence background from Raman spectra. The high-frequency modulation of the analyzed sample was combined with a phase-sensitive photomultiplier that could shift phase by $90°$ (58, 59). A monochromator was coupled to the photomultiplier in order to obtain the full spectrum but the spectral acquisition is slow because only the data at one wavenumber can be acquired a time with the single-channel photomultiplier tube (59).

Wavelength-Domain Methods

By Kasha's theory (63), the wavelength of a Raman peak closely follows the wavelength of the excitation source, whereas the fluorescence peak wavelength does not vary significantly with the excitation wavelength. The wavelength-domain methods take advantage of this theory to enhance very weak Raman signals dominated by fluorescence while removing the fluorescence (64). Common wavelength-domain methods include SERDS, wavelength-modulated Raman spectroscopy, and subtracted shifted Raman spectroscopy (SSRS).

SERDS (15, 24) requires an excitation laser source with at least two different narrow emission lines spectrally separated (65). The resulting spectrum is the difference between the two Raman spectra excited by two slightly shifted laser lines. Because the fluorescence spectrum is insensitive to the slight shift in the excitation laser wavelength, the contribution of fluorescence in the resulting difference spectrum is canceled out by the differentiation. The raw difference spectra obtained by SERDS are not ready for routine spectral analysis. To retrieve the actual Raman spectrum, several mathematical methods can be used to reconstruct a normal Raman spectrum from the raw difference spectrum, such as band fitting (24), the deconvolution procedure (65, 66), and principal component analysis (67). All of these algorithms yield a Raman spectrum with improved spectral quality compared to the raw difference spectrum while significantly suppressing fluorescence background. The SERDS method offers several distinct advantages such as improved signal-to-noise ratio and shortened data acquisition (16). Additionally, strong fluorescence background as well as other sources of systematic or random noises can be effectively removed.

For SERDS, a laser source is required to produce at least two slightly shifted excitation wavelengths and the spectral separation between these two excitation wavelengths is around 10 cm^{-1} or smaller, which is similar to the full-width at half-maximum of Raman bands in most solid and liquid samples. In one SERDS system, a compact diode laser with two semiconductor gain media in separate laser cavities using two reflection Bragg gratings was used to achieve two laser wavelengths at 670.0 and 671.6 nm (68). Another compact microsystem with a 488-nm laser source, emitting at 487.61 and 487.91 nm by tuning the temperature, was utilized to obtain the Raman spectra of polystyrene sample

using the method of shifted excitation resonance Raman difference spectroscopy, which was based on the principle of SERDS (69). Recently, two diode lasers with different central wavelengths at 783 and 671 nm, each emitting laser lines at two slightly shifted wavelengths, combined with a miniature spectrometer have been separately used for the rapid and noninvasive in situ discrimination of selected meat species (67).

SERDS has been improved by several groups in recent years to implement multiple excitation wavelengths and a cost-effective system. Cooper et al. (70) utilized a distributed Bragg reflector GaAs diode laser, which was temperature-controlled around 25°C and operated at four sequentially shifted excitation wavelengths around 785 nm, to reduce noise and eliminate fluorescence background in a set of inexpensive and compact instrumentation. Recently, a low-cost solution using a light-emitting diode (LED) at 365 nm with a resolution of >100 cm^{-1} as the light source has been demonstrated for SERDS. In the system, a conventional dielectric bandpass filter at 370 nm with 10 nm full-width at half-maximum was added to select the discrete spectral lines from LED radiation. Moreover, in order to obtain SERDS spectra, the filter's angle relative to the direction of light propagation was tuned to vary the emission wavelength range (71). By sequentially using multiple excitation wavelengths, multi-excitation Raman spectroscopy could efficiently suppress fluorescence background in Raman signals (15) obtained from human tooth and skin tissues. A novel numerical method called expectation-maximization algorithm was applied for constructing the normal Raman spectrum from more than two slightly shifted spectra.

SERDS has been combined with Kerr gating to further reduce fluorescence background in Raman spectroscopy (72). The combination dramatically enhanced the fluorescence suppression performance, which allowed the detection of a Raman signal 10^6 times lower than the fluorescence background and a sensitivity reaching the shot noise level of the detector. As a demonstration of SERDS's application, SERD and the optical trapping technique have been integrated in a confocal micro-Raman spectroscopy system to detect single motile biological cells; for example, *E. coli* bacteria, yeast cells, and red blood cells in an aqueous culture medium. The system effectively removed stray light interference and strong fluorescence background from the single-cell Raman spectra (73). This system enabled real-time measurements by utilizing a tunable semiconductor diode laser near 785 nm for single-cell trapping and slightly shifting the laser wavelength via tuning the temperature for Raman excitation. SERD could also be used to remove fluorescence background from SERS spectra of pyrene in water (74). In this study, a microsystem diode laser with two slightly different emission wavelengths ($\lambda = 487.61$ nm and $\lambda = 487.91$ nm) and a spectral width <10 pm was employed to investigate the SERS activity of a naturally grown silver nanoparticle ensemble. A detection limit around 2 nM pyrene in water was achieved.

Wavelength-modulated Raman spectroscopy (WMRS) (75–77), which is similar to SERDS in principle, uses an excitation light source with a continuously modulated excitation wavelength and multichannel lock-in detection to suppress fluorescence background (75). WMRS effectively distinguishes the Raman signal from fluorescence background by synchronizing a lock-in detector with the modulated excitation source. The WMRS technique takes advantage of the fact that fluorescence background is unchanged, whereas the periodical modulation of the excitation wavelength also modulates the Raman wavelengths.

De Luca et al. (75) analyzed WMRS Raman signal from a sample consisting of 2-μm polystyrene beads suspended in a fluorescent dye solution, as a function of the modulation rate of the excitation wavelength. In this study, the excitation wavelength was

continuously modulated from 0.03 to 0.4 Hz and multichannel lock-in detection was used to collect the retrieved differential spectra online. The signal-to-noise ratio of Raman signals obtained using WMRS at 0.4 Hz was three times higher than that using SERDS.

WMRS has been applied to the investigation of biological samples. Autofluorescence suppression using a wavelength-modulated excitation technique based on the principle of WMRS was utilized to collect wavelength-modulated Raman spectra from 697 individual circulating tumor cells (78) that consisted of acute myeloid leukaemia cells (OCI-AML3), breast tumor cells BT-20 and MCF-7, and leukocytes from patients' blood. The signal-to-noise ratio of each Raman spectrum obtained using the wavelength-modulated excitation technique was higher than that of the normal Raman spectrum after averaging. WMRS was also applied to the discrimination of urothelial cells and bladder cancer cells from human cell lines exposed to urine (79). Moreover, WMRS, via optimizing various parameters, has achieved a significant decrease in the acquisition time with a potential for high-throughput cell imaging and screening applications (77). WMRS was also an easily implementable and effective technique to reduce fluorescence background present in SERS spectra (80).

SSRS is also conceptually similar to SERDS. SSRS and WMRS have a significant experimental advantage over SERDS, which is the waiving in the requirement of a tunable laser source (15, 81). SSRS uses the slight change in the Raman spectrum achieved by employing two different grating positions while leaving the fluorescence background nearly unchanged. The subtracted spectra obtained from the raw data can be converted into a more recognizable and conventional form by various algorithms, such as the iterative fitting of appropriate double Lorentzian functions (42, 81). SSRS has been used to eliminate strong fluorescence background in real ancient objects over a supporting matrix, such as a textile or parchment, to identify small amounts of organic dyes and lakes (82). The main limitation of SSRS is that the subtracted spectra generated out of the raw data need further processing to be converted to a recognizable conventional form and they may contain spurious bands.

Computational Methods of Fluorescence Background Removal for Spectral Postprocessing

In addition to experimental methods for fluorescence suppression, computational methods have been widely adopted to postprocess measured Raman spectra directly to remove the fluorescence background. The most often used computational methods are based on polynomial fitting (26, 27, 83), wavelet transform (84–86), and derivatives (29, 87, 88).

The principle of the polynomial fitting method is that the fluorescence spectrum can be fit to a low-order polynomial (83) and then subtracted from the Raman spectrum. This is reasonable because fluorescence changes much slower than the Raman signal in the spectral dimension. The advantage of this method is that the original shapes of Raman peaks can be maintained after background subtraction. However, the optimal choice of order for polynomial fitting varies and the performance depends on the user's experience (89). Therefore, it is difficult to achieve an optimal fit if the intrinsic fluorescence of a sample is unknown.

The method of wavelet transform is based on the fact that the fluorescence background is mainly composed of slowly changing and low-frequency components compared to the Raman signal (84). The measured spectrum can be decomposed into different frequency components first and then those low-frequency components corresponding to fluorescence background can be removed. Unfortunately, a large number of parameters need

to be set in this method; for example, basis functions, transformation levels, and coefficients to remove, which makes it difficult to optimize those parameters and often time consuming (85).

The method of derivatives is probably the simplest and most robust way for fluorescence background removal and it shows significant advantages in computation. The derivatives of the fluorescence background are always smaller in magnitude than those of Raman peaks; thus, taking the derivative of a measured Raman spectrum will eliminate the background components irrespective of their magnitudes and thus enhance the sharp Raman signal (90). However, high-frequency noises are often amplified by this method as well and the spectrum can be distorted because of the derivative process. The distortion causes the derivative spectrum to be different from the original spectrum in appearance, which makes the interpretation of the derivative spectrum difficult (88).

There also exist some other computational methods for fluorescence suppression, such as peak detection (91, 92), principal component analysis (25, 93), Fourier transform filtering (27, 28), and manual baseline correction (94). However, they are relatively less often used compared with the above three major types of computational methods.

Other Methods

There are several other methods for suppressing fluorescence emission that do not belong to any of the above categories. One such technique is based on the different responses in Raman scattering and fluorescence to polarization modulation. Because Raman scattering in symmetric vibrations is tightly related to the polarization of incident light (95), the polarization dependence on the excitation light can be useful in discrimination between Raman molecules with polarized Raman bands and fluorophores with low fluorescence anisotropy. Angel et al. (38) introduced a polarization modulation technique to suppress fluorescence. In this study, a polarizer chopper synchronized with a lock-in amplifier was used to separate nonpolarized fluorescence background and the polarized Raman spectrum. The fluorescence signal was significantly reduced and the Raman spectrum was detected for rhodamine 6G at a concentration of 1 nM in ethanol solution. However, this technique will become ineffective if the parallel-polarized fluorescence with the polarization along the direction of the excitation light is not negligible (15).

Another technique using a spatially engineered excitation beam—for example, Laguerre-Gaussian beam or holey-Gaussian beam—instead of the standard Gaussian beam (39) was shown to significantly suppress fluorescence background and allow fast Raman signal acquisition, subsequently lower photo-induced damage risk. The configurations of the Laguerre-Gaussian beam and holey-Gaussian beam could detect specific Raman peaks with fluorescence background reduced by 3.4 and 2.2 times, respectively, compared to the configuration of the Gaussian beam. It should be noted that this method only allows the partial removal of fluorescence background. Regarding the mechanism behind this method, it was speculated by the authors that the Raman signal was collected from the dark core region of the Laguerre-Gaussian beam or holey-Gaussian beam, in which the trapped object was partly located, but fluorescence cannot be efficiently collected from this region. To reject the fluorescence signal from a substrate, another approach called dark-field Raman microscopy was proposed, in which the excitation beam converges above the sample's surface while the collection optics is focused on the sample's surface (40). In this configuration, the fluorescence from 5-μm-thick breast tissue on a glass substrate was lowered by three- to fourfold.

Photobleaching by pulsed laser excitation has been used to suppress fluorescence background in the Raman spectra of solid materials. Hamaguchi et al. (41) stated that

high-energy laser pulses would cause the photoexcitation time, which is the time taken by a molecule to jump from the ground state to the excited state by the pulsed laser, to be much shorter than the fluorescence recovery time, which is the time taken by a molecule to return from the excited state to the ground state, resulting in complete depletion of molecules in the ground state. This will quench fluorescence while the Raman scattering process remains unchanged. It was demonstrated that the Raman-to-fluorescence ratio of DNA tetramer and protein samples was increased by a factor of 10 to 100 by photobleaching (41). In another study (42), photobleaching of painted textiles was achieved by prolonged pulse laser irradiation, which improved the ratio of Raman signal to noise by 10-fold after photobleaching for 2 h. The photobleaching method has been also used to reduce fluorescence background in the Raman measurements of automotive paints (96). Constant sample irradiation for a long period of time prior to Raman measurements allows fluorescence to be quenched significantly, which made pigment identification using Raman spectroscopy possible. It should be pointed out that photobleaching by long laser irradiation may result in the long-term damage to samples, especially for fragile historic artifacts. Though the fluorescence photobleaching method used by Hamaguchi et al. (41), due to the mechanism that laser pulses induced the transient optical depletion of fluorophore molecules on the ground state, should be nondestructive, the method reported by MacDonald and Wyeth (42) is likely destructive due to the prolonged continuous irradiation. Furthermore, the photobleaching method could be used in liquid core optical fiber waveguides as well to suppress fluorescence background in the Raman spectra of liquid samples by more than two orders of magnitude (97).

Comparison Among the Major Experimental and Computational Methods

To facilitate the selection of a proper method for a particular application, Table 1 compares the major fluorescence suppression methods in terms of cost, performance, and most important advantage(s) or limitation(s). It needs to be highlighted that such comparison is highly qualitative because the relevant data are either extracted from different papers in the literature, in which the experimental configuration may vary significantly from one to another, or based on our own experience. The table is only intended to serve as the initial evaluation of methods in different categories, for which detailed validation is highly recommended. Among these methods, it can be seen that applying one or more of the computational methods for fluorescence background removal is the most cost-effective choice. However, this category of methods is limited in performance, especially for weak Raman signals, because they often create artifacts in spectra. For the best fluorescence suppression performance, a time-domain method, especially the one with a gated streak camera (49), appears to be the proper choice; however, the requirements of a pulsed laser with a short pulse width and a detector with a short time gate width make such a system very expensive. The intermediate choice, which is a tradeoff between cost and performance, may be various wavelength-domain methods, which can be implemented with a diode laser or LED and a normal Raman spectrometer (70, 71). It should be highlighted that various computational methods could be combined with the first three categories of experimental methods to further improve performance.

Discussion and Conclusion

From a practical point of view, expensive time-domain and frequency-domain methods for Raman spectroscopy alone may find their uses only in a small number of research

Table 1.

Comparison among the major categories of fluorescence suppression methods in terms of cost, performance, and important advantage(s) or limitation(s). The performance evaluation was based on the typical improvement in the Raman-to-fluorescence ratio reported in relevant papers and the cost evaluation was based on our own experience

Methods	Cost	Performance	Remarks
Time-domain methods (18–20)	Medium to high	High (49)	Advantages: Capable of separating the Raman signal from the deep layer and that from the superficial layer and minimizing the effect of photon scattering in thick samples (98). Effective in reducing statistical noise (22). Limitations: Ineffective when the fluorescence lifetime is comparable to the excitation pulse duration (65). Spectral resolution decreasing with the laser pulse width (15). Requiring excessively high pulse energies in the Kerr gating method (45).
Frequency-domain methods (21–23)	Medium to high	Medium (23)	Limitations: Requiring strong Raman signals to overcome fluorescence background (23). Unable to suppress fluorescence in Raman measurements with a large bandwidth (22, 23).
Wavelength-domain methods (79, 81)	Medium	Medium (75)	Advantage: Requiring moderate modification of an ordinary Raman system (80). Limitations: Requiring further complex data processing to obtain normal Raman spectra (81). Strong dependence of spectral reproduction on the noise level in the raw spectra (99).
Computational methods (25–29)	Low	Medium to high (83)	Advantage: The method can be usually tuned to preserve specific spectral features after the subtraction of background (83, 84). Limitations: The optimal choices of key parameters depend on the user's experience (85, 89). The data processing can be time consuming (85) and the resulting spectrum could be distorted such as in the derivative method (88) and may contain artifacts especially in weak Raman signals.

applications requiring exceptional performance in fluorescence suppression such as when performing bone characterization through the skin (19). However, given that these methods can often measure fluorescence lifetime after moderate revision in the system configuration, they may find a broader range of applications when they are further developed to combine both Raman spectroscopy and fluorescence lifetime measurements. The fluorescence lifetime technique alone has been explored for a variety of purposes such as cancer diagnosis (100, 101). In most other applications, one of those wavelength-domain methods is likely a good choice that makes a compromise between the cost and performance. In this category of methods, a mathematical method, such as principal component analysis, that can effectively estimate the corresponding normal Raman spectrum from a difference spectrum, is needed for common use (76). In addition, various computational methods for fluorescence background removal can always be tuned for a particular application to enhance the performance of fluorescence suppression without significantly increasing the cost if needed.

The fluorescence suppression techniques discussed in this article were demonstrated mostly for point scanning in single-channel measurements. When a large sample needs to be examined, Raman measurements at many pixels will be required. In this case, a few of the above methods based on 2D detector arrays can be potentially used for line scanning while still keeping a reasonable spectral resolution or for 2D imaging but at the cost of sacrificing the spectral resolution to speed up Raman data acquisition. To achieve even faster Raman imaging and still obtain the full Raman spectrum at every pixel, one potential way is to combine one of the above fluorescence suppression techniques with a fast Raman imaging technique based on narrow band imaging and spectral reconstruction (102). This new Raman measurement technique suitable for imaging has been demonstrated to be effective in both spontaneous Raman spectroscopy and surface-enhanced Raman spectroscopy. It is expected to improve the speed of Raman imaging by a few orders of magnitude when the full capability is realized in an imaging system.

In this article, we have reviewed several techniques for suppressing the strong fluorescence background in Raman spectroscopy to expand its use in many applications; for example, agriculture (103) and food (104), tissue engineering (14, 51, 89), and clinical diagnosis (105). These techniques take advantage of the differences between Raman and fluorescence signals in the time domain, the frequency domain, and the wavelength domain, which can thus be applied to various scenarios. This survey pays special attention to the fundamental principles of each category of methods in addition to the recent advances. Moreover, those major categories of techniques are compared to each other in terms of cost and performance in the hope to guide interested readers to select proper methods for specific applications. We also expect one or a few of these experimental methods to be more commonly accepted in the near future once they become user-friendly and demonstrate consistent performance in different applications.

Funding

References

1. Gardiner, D.J. (1989) *Practical Raman Spectroscopy*. Springer-Verlag: Berlin, Germany.
2. Lakowicz, J.R. (2006) *Principles of Fluorescence Spectroscopy*. 3rd ed. Springer: New York.
3. Kohl, I., Winkel, K., Bauer, M., Liedl, K.R., Loerting, T., and Mayer, E. (2009) Raman spectroscopic study of the phase transition of amorphous to crystalline beta-carbonic acid. *Angew. Chem. Int. Ed.*, 48 (15): 2690–2694.
4. Kobayashi, M., Kaneko, F., Sato, K., and Suzuki, M. (1986) Vibrational spectroscopic study on polymorphism and order-disorder phase-transition in oleic-acid. *J. Phys. Chem.*, 90 (23): 6371–6378.
5. Taylor, L.S. and Zografi, G. (1998) The quantitative analysis of crystallinity using FT-Raman spectroscopy. *Pharmaceut. Res.*, 15 (5): 755–761.
6. Ong, Y.H., Lim, M., and Liu, Q. (2012) Comparison of principal component analysis and biochemical component analysis in Raman spectroscopy for the discrimination of apoptosis and necrosis in K562 leukemia cells. *Optic. Express*, 20 (22): 25041–25043.
7. Ojeda, J.F., Xie, C.G., Li, Y.Q., Bertrand, F.E., Wiley, J., and McConnell, T.J. (2006) Chromosomal analysis and identification based on optical tweezers and Raman spectroscopy. *Optic. Express*, 14 (12): 5385–5393.
8. Wood, B.R., Tait, B. and McNaughton, D. (2001) Micro-Raman characterisation of the R to T state transition of haemoglobin within a single living erythrocyte. *Biochim. Biophys. Acta Mol. Cell Res.*, 1539 (1–2): 58–70.
9. Yuen, C. and Liu, Q. (2012) Magnetic field enriched surface enhanced resonance Raman spectroscopy for early malaria diagnosis. *J. Biomed. Optic.*, 17 (1): 017005
10. Webster, G.T., Tilley, L., Deed, S., McNaughton, D., and Wood, B.R. (2008) Resonance Raman spectroscopy can detect structural changes in haemozoin (malaria pigment) following incubation with chloroquine in infected erythrocytes. *FEBS Lett.*, 582 (7): 1087–1092.
11. Andrade, P.O., Bitar, R.A., Yassoyama, K., Martinho, H., Santo, A.M.E., Bruno, P.M., and Martin, A.A. (2007) Study of normal colorectal tissue by FT-Raman spectroscopy. *Anal. Bioanal. Chem.*, 387 (5): 1643–1648.
12. Bitar, R.A., Martinho, H.D.S., Tierra-Criollo, C.J., Ramalho, L.N.Z., Netto, M.M., and Martin, A.A. (2006) Biochemical analysis of human breast tissues using Fourier-transform Raman spectroscopy. *J. Biomed. Optic.*, 11 (5): 054001.
13. Krishna, C.M., Prathima, N.B., Malini, R., Vadhiraja, B.M., Bhatt, R.A., Fernandes, D.J., Kushtagi, P., Vidyasagar, M.S., and Kartha, V.B. (2006) Raman spectroscopy studies for diagnosis of cancers in human uterine cervix. *Vib. Spectros.*, 41 (1): 136–141.
14. Carden, A. and Morris, M.D. (2000) Application of vibrational spectroscopy to the study of mineralized tissues (review). *J. Biomed. Optic.*, 5 (3): 259–268.
15. Martins, M.A.D., Ribeiro, D.G., dos Santos, E.A.P., Martin, A.A., Fontes, A., and Martinho, H.D. (2010) Shifted-excitation Raman difference spectroscopy for in vitro and in vivo biological samples analysis. *Biomed. Optic. Express*, 1 (2): 617–626.
16. Kostamovaara, J., Tenhunen, J., Kogler, M., Nissinen, I., Nissinen, J., and Keranen, P. (2013) Fluorescence suppression in Raman spectroscopy using a time-gated CMOS SPAD. *Optic. Express*, 21 (25): 31632–31645.
17. Hanlon, E.B., Manoharan, R., Koo, T.W., Shafer, K.E., Motz, J.T., Fitzmaurice, M., Kramer, J.R., Itzkan, I., Dasari, R.R., and Feld, M.S. (2000) Prospects for in vivo Raman spectroscopy. *Phys. Med. Biol.*, 45 (2): R1–R59.
18. Burgess, S. and Shepherd, I.W. (1977) Fluorescence suppression in time-resolved Raman-spectra. *J. Phys. E Sci. Instrum.*, 10 (6): 617–620.
19. Ariese, F., Meuzelaar, H., Kerssens, M.M., Buijs, J.B., and Gooijer, C. (2009) Picosecond Raman spectroscopy with a fast intensified CCD camera for depth analysis of diffusely scattering media. *Analyst*, 134 (6): 1192–1197.
20. Goncharov, A.F. and Crowhurst, J.C. (2005) Pulsed laser Raman spectroscopy in the laser-heated diamond anvil cell. *Rev. Sci. Instrum.*, 76 (6): 063905.

21. Genack, A.Z. (1985) Electro-optic phase-sensitive detection of optical-emission and scattering. *Appl. Phys. Lett.*, 46 (4): 341–343.
22. Demas, J.N. and Keller, R.A. (1985) Enhancement of luminescence and Raman-spectroscopy by phase-resolved background suppression. *Anal. Chem.*, 57 (2): 538–545.
23. Wirth, M.J. and Chou, S.H. (1988) Comparison of time and frequency-domain methods for rejecting fluorescence from Raman-spectra. *Anal. Chem.*, 60 (18): 1882–1886.
24. Shreve, A.P., Cherepy, N.J., and Mathies, R.A. (1992) Effective rejection of fluorescence interference in Raman-spectroscopy using a shifted excitation difference technique. *Appl. Spectros.*, 46 (4): 707–711.
25. Hasegawa, T., Nishijo, J., and Umemura, J. (2000) Separation of Raman spectra from fluorescence emission background by principal component analysis. *Chem. Phys. Lett.*, 317 (6): 642–646.
26. Zhao, J., Lui, H., McLean, D.I. and Zeng, H. (2007) Automated autofluorescence background subtraction algorithm for biomedical Raman spectroscopy. *Appl. Spectros.*, 61 (11): 1225–1232.
27. Lieber, C.A. and Mahadevan-Jansen, A. (2003) Automated method for subtraction of fluorescence from biological Raman spectra. *Appl. Spectros.*, 57 (11): 1363–1367.
28. Mosierboss, P.A., Lieberman, S.H., and Newbery, R. (1995) Fluorescence rejection in Raman-spectroscopy by shifted-spectra, edge-detection, and FFT filtering techniques. *Appl. Spectros.*, 49 (5): 630–638.
29. Zhang, D.M. and Ben-Amotz, D. (2000) Enhanced chemical classification of Raman images in the presence of strong fluorescence interference. *Appl. Spectros.*, 54 (9): 1379–1383.
30. Yuen, C. and Liu, Q. (2013) Towards in vivo intradermal surface enhanced Raman scattering (SERS) measurements: Silver coated microneedle based SERS probe. *J. Biophoton.*, 2013: 683–689.
31. Campion, A. and Kambhampati, P. (1998) Surface-enhanced Raman scattering. *Chem. Soc. Rev.*, 27 (4): 241–250.
32. Dong, L., Ye, F., Hu, J., Popov, S., Friberg, A.T. and Muhammed, M. (2011) Fluorescence quenching and photobleaching in Au/Rh6G nanoassemblies: Impact of competition between radiative and non-radiative decay. *J. Eur. Opt. Soc.*, 6: 11019.
33. Morris, M.D. (1979) Resonance Raman-spectroscopy—Current applications and prospects. *Anal. Chem.*, 51 (2): 182A–192A.
34. Efremov, E.V., Ariese, F., and Gooijer, C. (2008) Achievements in resonance Raman spectroscopy review of a technique with a distinct analytical chemistry potential. *Anal. Chim. Acta*, 606 (2): 119–134.
35. Robert, B. (2009) Resonance Raman spectroscopy. *Photosynth. Res.*, 101 (2–3): 147–155.
36. Evans, C.L. and Xie, X.S. (2008) Coherent anti-Stokes Raman scattering microscopy: Chemical imaging for biology and medicine. *Annu. Rev. Anal. Chem.*, 1: 883–909.
37. Kukura, P., McCamant, D.W., and Mathies, R.A. (2007) Femtosecond stimulated Raman spectroscopy. *Annu. Rev. Phys. Chem.*, 58: 461–488.
38. Angel, S.M., Dearmond, M.K., Hanck, K.W., and Wertz, D.W. (1984) Computer-controlled instrument for the recovery of a resonance Raman-spectrum in the presence of strong luminescence. *Anal. Chem.*, 56 (14): 3000–3001.
39. Cormack, I.G., et al. (2007) Fluorescence suppression within Raman spectroscopy using annular beam excitation. *Appl. Phys. Lett.*, 91 (2): 023903.
40. Schulmerich, M.V., et al. (2010) Dark field Raman microscopy. *Anal. Chem.*, 82 (14): 6273–6280.
41. Hamaguchi, H., Tahara, T., and Tasumi, M. (1987) Suppression of luminescence background in Raman-spectroscopy by means of transient optical depletion of causal impurity molecules. *Appl. Spectros.*, 41 (8): 1265–1268.
42. Macdonald, A.M. and Wyeth, P. (2006) On the use of photobleaching to reduce fluorescence background in Raman spectroscopy to improve the reliability of pigment identification on painted textiles. *J. Raman Spectros.*, 37 (8): 830–835.
43. Sahoo, S.K., Umapathy, S., and Parker, A.W. (2011) Time-resolved resonance Raman spectroscopy: Exploring reactive intermediates. *Appl. Spectros.*, 65 (10): 1087–1115.

44. Becker, W. (2012) Fluorescence lifetime imaging—Techniques and applications. *J. Microsc.*, 247 (2): 119–136.

45. Matousek, P., Towrie, M., Stanley, A., and Parker, A.W. (1999) Efficient rejection of fluorescence from Raman spectra using picosecond Kerr gating. *Appl. Spectros.*, 53 (12): 1485–1489.

46. Watanabe, J., Kinoshita, S., and Kushida, T. (1985) Fluorescence rejection in Raman-spectroscopy by a gated single-photon counting method. *Rev. Sci. Instrum.*, 56 (6): 1195–1198.

47. Martyshkin, D.V., Ahuja, R.C., Kudriavtsev, A., and Mirov, S.B. (2004) Effective suppression of fluorescence light in Raman measurements using ultrafast time gated charge coupled device camera. *Rev. Sci. Instrum.*, 75 (3): 630–635.

48. Efremov, E.V., Buijs, J.B., Gooijer, C., and Ariese, F. (2007) Fluorescence rejection in resonance Raman spectroscopy using a picosecond-gated intensified charge-coupled device camera. *Appl. Spectros.*, 61 (6): 571–578.

49. Tahara, T. and Hamaguchi, H.O. (1993) Picosecond Raman-spectroscopy using a streak camera. *Appl. Spectros.*, 47 (4): 391–398.

50. Matousek, P., et al. (2001) Fluorescence suppression in resonance Raman spectroscopy using a high-performance picosecond Kerr gate. *J. Raman Spectros.*, 32 (12): 983–988.

51. Morris, M.D., Matousek, P., Towrie, M., Parker, A.W., Goodship, A.E., and Draper, E.R.C. (2005) Kerr-gated time-resolved Raman spectroscopy of equine cortical bone tissue. *J. Biomed. Optic.*, 10 (1): 014014.

52. Everall, N., Hahn, T., Matousek, P., Parker, A.W., and Towrie, M. (2001) Picosecond time-resolved Raman spectroscopy of solids: Capabilities and limitations for fluorescence rejection and the influence of diffuse reflectance. *Appl. Spectros.*, 55 (12): 1701–1708.

53. Sinfield, J.V., Colic, O., Fagerman, D., and Monwuba, C. (2010) A low cost time-resolved Raman spectroscopic sensing system enabling fluorescence rejection. *Appl. Spectros.*, 64(2): 201–210.

54. Litwiller, D. (2002) CCD vs. CMOS: The battle cools off. *Photon. Spectra*, 36 (1): 102–103.

55. Zlatanski, M., Uhring, W., Le Normand, J.P., Zint, C.V., and Mathiot, D. (2010) Streak camera in standard (Bi)CMOS (bipolar complementary metal-oxide-semiconductor) technology. *Meas. Sci. Tech.*, 21 (11): 115203–115214.

56. Hain, R., Kahler, C.J., and Tropea, C. (2007) Comparison of CCD, CMOS and intensified cameras. *Exp. Fluid.*, 42 (3): 403–411.

57. Bright, F.V. and Hieftje, G.M. (1986) A new technique for the elimination of fluorescence interference in Raman-spectroscopy. *Appl. Spectros.*, 40 (5): 583–587.

58. Rusciano, G., De Luca, A.C., Sasso, A., and Pesce, G. (2006) Phase-sensitive detection in Raman tweezers. *Appl. Phys. Lett.*, 89 (26): 261116.

59. Rusciano, G., De Luca, A.C., Sasso, A. and Pesce, G. (2007) Enhancing Raman tweezers by phase-sensitive detection. *Anal. Chem.*, 79 (10): 3708–3715.

60. Genack, A.Z. (1984) Fluorescence suppression by phase-resolved modulation Raman-scattering. *Anal. Chem.*, 56 (14): 2957–2960.

61. Bright, F.V. (1988) Multicomponent suppression of fluorescent interferants using phase-resolved Raman-spectroscopy. *Anal. Chem.*, 60 (15): 1622–1623.

62. Jameson, D.M., Gratton, E., and Hall, R.D. (1984) The measurement and analysis of heterogeneous emissions by multifrequency phase and modulation fluorometry. *Appl. Spectros. Rev.*, 20 (1): 55–106.

63. Kasha, M. (1950) Characterization of electronic transitions in complex molecules. *Discuss. Faraday Soc.*, 1950 (9): 14–19.

64. McCain, S.T., Willett, R.M., and Brady, D.J. (2008) Multi-excitation Raman spectroscopy technique for fluorescence rejection. *Optic. Express*, 16 (15): 10975–10991.

65. Zhao, J., Carrabba, M.M., and Allen, F.S. (2002) Automated fluorescence rejection using shifted excitation Raman difference spectroscopy. *Appl. Spectros.*, 56 (7): 834–845.

66. Matousek, P., Towrie, M., and Parker, A.W. (2005) Simple reconstruction algorithm for shifted excitation Raman difference spectroscopy. *Appl. Spectros.*, 59 (6): 848–851.

67. Sowoidnich, K. and Kronfeldt, H.D. (2012) Shifted excitation Raman difference spectroscopy at multiple wavelengths for in-situ meat species differentiation. *Appl. Phys. B Laser. Optic.*, 108 (4): 975–982.

68. Maiwald, M., M., Schmidt, H., Sumpf, B., Erbert, G., Kronfeldt, H.D., and Trankle, G. (2009) Microsystem 671 nm light source for shifted excitation Raman difference spectroscopy. *Appl. Optic.*, 48 (15): 2789–2792.

69. Maiwald, M., et al. (2009) Microsystem light source at 488 nm for shifted excitation resonance Raman difference spectroscopy. *Appl. Spectros.*, 63 (11): 1283–1287.

70. Cooper, J.B., Abdelkader, M., and Wise, K.L. (2013) Sequentially shifted excitation Raman spectroscopy: Novel algorithm and instrumentation for fluorescence-free Raman spectroscopy in spectral space. *Appl. Spectros.*, 67 (8): 973–984.

71. Adami, R. and Kiefer, J. (2013) Light-emitting diode based shifted-excitation Raman difference spectroscopy (LED-SERDS). *Analyst*, 138 (21): 6258–6261.

72. Matousek, P., Towrie, M., and Parker, A.W. (2002) Fluorescence background suppression in Raman spectroscopy using combined Kerr gated and shifted excitation Raman difference techniques. *J. Raman Spectros.*, 33 (4): 238–242.

73. Xie, C.G. and Li, Y.Q. (2003) Confocal micro-Raman spectroscopy of single biological cells using optical trapping and shifted excitation difference techniques. *J. Appl. Phys.*, 93 (5): 2982–2986.

74. Kwon, Y.H., Ossig, R., Hubenthal, F., and Kronfeldt, H.D. (2012) Influence of surface plasmon resonance wavelength on SERS activity of naturally grown silver nanoparticle ensemble. *J. Raman Spectros.*, 43 (10): 1385–1391.

75. De Luca, A.C., Mazilu, M., Riches, A., Herrington, C.S., and Dholakia, K. (2010) Online fluorescence suppression in modulated Raman spectroscopy. *Anal. Chem.*, 82 (2): 738–745.

76. Mazilu, M., De Luca, A.C., Riches, A., Herrington, C.S., and Dholakia, K. (2010) Optimal algorithm for fluorescence suppression of modulated Raman spectroscopy. *Optic. Express*, 18 (11): 11382–11395.

77. Praveen, B.B., Mazilu, M., Marchington, R.F., Herrington, C.S., Riches, A., and Dholakia, K. (2013) Optimisation of wavelength modulated Raman spectroscopy: Towards high throughput cell screening. *PLos One*, 8 (6): e67211.

78. Dochow, S., Bergner, N., Krafft, C., Clement, J., Mazilu, M., Praveen, B.B., Ashok, P.C., Marchington, R., Dholakia, K., and Popp, J. (2013) Classification of Raman spectra of single cells with autofluorescence suppression by wavelength modulated excitation. *Anal. Meth.*, 5 (18): 4608–4614.

79. Canetta, E., Mazilu, M., De Luca, A.C., Carruthers, A.E., Dholakia, K., Neilson, S., Sargeant, H., Briscoe, T., Herrington, C.S. and Riches, A.C. (2011) Modulated Raman spectroscopy for enhanced identification of bladder tumor cells in urine samples. *J. Biomed. Optic.*, 16 (3): 037002

80. Praveen, B.B., Steuwe, C., Mazilu, M., Dholakia, K., and Mahajan, S. (2013) Wavelength modulated surface enhanced (resonance) Raman scattering for background-free detection. *Analyst*, 138 (10): 2816–2820.

81. Bell, S.E.J., Bourguignon, E.S.O., and Dennis, A. (1998) Analysis of luminescent samples using subtracted shifted Raman spectroscopy. *Analyst*, 123 (8): 1729–1734.

82. Rosi, F., Paolantoni, M., Clementi, C., Doherty, B., Miliani, C., Brunetti, B.G., and Sgamellotti, A. (2010) Subtracted shifted Raman spectroscopy of organic dyes and lakes. *J. Raman Spectros.*, 41 (4): 452–458.

83. Mazet, V., Carteret, C., Brie, D., Idier, J., and Humbert, B. (2005) Background removal from spectra by designing and minimising a non-quadratic cost function. *Chemometr. Intell. Lab. Syst.*, 76 (2): 121–133.

84. Galloway, C.M., Le Ru, E.C., and Etchegoin, P.G. (2009) An iterative algorithm for background removal in spectroscopy by wavelet transforms. *Appl. Spectros.*, 63 (12): 1370–1376.

85. Hu, Y.G., Jiang, T., Shen, A.G., Li, W., Wang, X.P. and Hu, J.M. (2007) A background elimination method based on wavelet transform for Raman spectra. *Chemometr. Intell. Lab. Syst.*, 85 (1): 94–101.

86. Ramos, P.M. and Ruisanchez, I. (2005) Noise and background removal in Raman spectra of ancient pigments using wavelet transform. *J. Raman Spectros.*, 36 (9): 848–856.

87. O'Grady, A., Dennis, A.C., Denvir, D., McGarvey, J.J., and Bell, S.E.J. (2001) Quantitative Raman spectroscopy of highly fluorescent samples using pseudosecond derivatives and multivariate analysis. *Anal. Chem.*, 73 (9): 2058–2065.

88. Leger, M.N. and Ryder, A.G. (2006) Comparison of derivative preprocessing and automated polynomial baseline correction method for classification and quantification of narcotics in solid mixtures. *Appl. Spectros.*, 60 (2): 182–193.

89. Cao, A., Pandya, A.K., Serhatkulu, G.K., Weber, R.E., Dai, H., Thakur, J.S., Naik, V.M., Naik, R., Auner, G.W., Rabah, R., and Freeman, D.C. (2007) A robust method for automated background subtraction of tissue fluorescence. *J. Raman Spectros.*, 38 (9): 1199–1205.

90. Schulze, G., Jirasek, A., Yu, M.M.L., Lim, A., Turner, R.F.B., and Blades, M.W. (2005) Investigation of selected baseline removal techniques as candidates for automated implementation. *Appl. Spectros.*, 59 (5): 545–574.

91. Baek, S.J., Park, A., Kim, J., Shen, A.G., and Hu, J.M. (2009) A simple background elimination method for Raman spectra. *Chemometr. Intell. Lab. Syst.*, 98 (1): 24–30.

92. Zhang, Z.M., Chen, S., Liang, Y.Z., Liu, Z.X., Zhang, Q.M., Ding, L.X., Ye, F., and Zhou, H. (2010) An intelligent background-correction algorithm for highly fluorescent samples in Raman spectroscopy. *J. Raman Spectros.*, 41 (6): 659–669.

93. Palacky, J., Mojzes, P., and Bok, J. (2011) SVD-based method for intensity normalization, background correction and solvent subtraction in Raman spectroscopy exploiting the properties of water stretching vibrations. *J. Raman Spectros.*, 42 (7): 1528–1539.

94. Jirasek, A., Schulze, G., Yu, M.M.L., Blades, M.W., and Turner, R.F.B. (2004) Accuracy and precision of manual baseline determination. *Appl. Spectros.*, 58 (12): 1488–1499.

95. McCreery, R.L. (2000) *Raman Spectroscopy for Chemical Analysis*. Wiley-Interscience: New York.

96. Zięba-Palus, J. and Michalska, A. (2014) Photobleaching as a useful technique in reducing of fluorescence in Raman spectra of blue automobile paint samples. *Vib. Spectros.*, 74: 6–12.

97. Pelletier, M.J. and Altkorn, R. (2000) Efficient elimination of fluorescence background from Raman spectra collected in a liquid core optical fiber. *Appl. Spectros.*, 54 (12): 1837–1841.

98. Matousek, P., Everall, N., Towrie, M., and Parker, A.W. (2005) Depth profiling in diffusely scattering media using Raman spectroscopy and picosecond Kerr gating. *Appl. Spectros.*, 59 (2): 200–205.

99. Osticioli, I., Zoppi, A., and Castellucci, E.M. (2007) Shift-excitation Raman difference spectroscopy-difference deconvolution method for the luminescence background rejection from Raman spectra of solid samples. *Appl. Spectros.*, 61 (8): 839–844.

100. Berezin, M.Y. and Achilefu, S. (2010) Fluorescence lifetime measurements and biological imaging. *Chem. Rev.*, 110 (5): 2641–2684.

101. Tadrous, P.J., Siegel, J., French, P.M., Shousha, S., Lalani el, N., and Stamp, G.W. (2003) Fluorescence lifetime imaging of unstained tissues: Early results in human breast cancer. *J Pathol.*, 199 (3): 309–317.

102. Chen, S., Ong, Y.H., and Liu, Q. (2013) Fast reconstruction of Raman spectra from narrowband measurements based on Wiener estimation. *J. Raman Spectros.*, 44 (6): 875–881.

103. Pulgarin, J.A.M., Bermejo, L.F.G., and Rodriguez, S.B. (2013) Direct determination of gibberellic acid in tomato and fruit by using photochemically induced fluorescence. *J. Agr. Food Chem.*, 61 (41): 9769–9775.

104. Ryvolova, M., Taborsky, P., Vrabel, P., Krasensky, P., and Preisler, J. (2007) Sensitive determination of erythrosine and other red food colorants using capillary electrophoresis with laser-induced fluorescence detection. *J. Chrom.*, 1141 (2): 206–211.

105. Barberia, E., Maroto, M., Arenas, M., and Silva, C.C. (2008) A clinical study of caries diagnosis with a laser fluorescence system. *J. Am. Dent. Assoc.*, 139 (5): 572–579.